V/f Control Method for Pulsating Torque Reduction in a Single Phase Induction Motor

Seung-Cheol Choi[1], Jung-Han Kim[1], Young-Doo Yoon[2], Chan-Ook Hong[1], Cheol-Hyun Park[1], and Joo-Hyun Cho[1]
[1] LS ELECTRIC, Korea
[2] Hanyang University, Korea

***Abstract*—In general, single-phase induction motors have main and auxiliary windings on the stator which is an asymmetrical circuit for the starting torque. Due to an asymmetrical stator circuit, the torque pulsation is generated with noise and loss. The paper proposes the open-loop V/f control method for reducing the torque pulsation in a single-phase induction motor. The proposed method uses a three-leg inverter and power sharing controllers without the start capacitor. The line-to-line voltages of a three-leg inverter correspond to two winding voltages, and the active power sharing of two windings is adjusted by the voltage ratio while the reactive power sharing is adjusted by the phase angle difference. With the proposed method, average active and reactive powers on the stator windings are equal and thus the torque pulsation is reduced in a single-phase induction motor. The effectiveness of the proposed method is validated by simulation and experimental results.**

***Index Terms*—open-loop V/f control, power sharing, single-phase induction motor, torque pulsation.**

I. Introduction

Single-phase induction motors (SPIMs) are widely used in low-power industrial and household applications such as pumps, fans, refrigerators, air conditioners, and so on. They are simple in structure and easy to repair. Small SPIMs are cheaper than similar power-rating three-phase motors. Therefore, low-power applications utilize SPIMs instead of three-phase motors because of low cost, ease of use and maintenance. On the contrary, there are several disadvantages including low efficiency, low power factor and torque pulsation. Also, an additional winding in most SPIMs is required for the starting torque when supplied with a fixed single-phase voltage source. As shown in Fig. 1, the SPIM has main and auxiliary windings displaced 90 electrical degrees on the stator. The capacitor-start induction motor has a capacitor in series with the auxiliary winding for the auto start-up. When the SPIM is connected to a single-phase AC power supply, the start capacitor produces stator currents with a phase angle difference for generating the rotating magnetic field [1], [2].

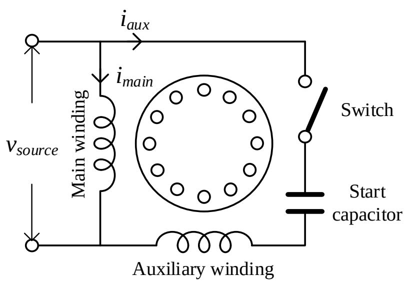

Fig. 1. Capacitor-start induction motor.

A voltage source inverter (VSI) is preferred in variable speed drive systems because variable voltage variable frequency (VVVF) operation offers not only energy savings but also soft run/stop capabilities. When the three-leg VSI drives the SPIM, the start capacitor is removed to prevent resonance problem and over current occurrence, as shown in Fig. 2, and the SPIM is considered an asymmetrical two-phase motor in which two stator windings have different impedances. For the SPIM drives, line-to-line voltages of a three-leg VSI are connected to main and auxiliary windings.

In most of the industrial applications, the open-loop volt/hertz (V/f) control is the one of widely used control methods for induction motor drives because of simplicity. In a general V/f control, various information regarding motor parameters isn't required except for nameplate values. It is a simple variable speed control technique which maintains the ratio of voltages to frequency from zero to rated speed without flux and current controllers. In symmetrical induction motors, the rotating magnetic field is kept uniform with the V/f control. However, SPIMs have an asymmetrical stator circuit consisting of main and auxiliary windings. Due to asymmetrical windings, it is difficult to produce a uniform circular rotating magnetic field with the two-phase balanced voltages shown in Fig. 3. Consequently, the distortion of rotating magnetic field generates torque pulsations. In [3], the unbalanced voltages are applied to stator windings for a uniform circular rotating magnetic field.

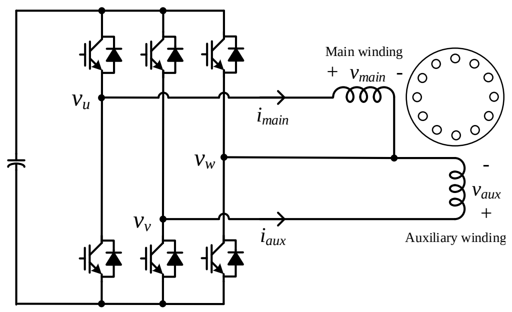

Fig. 2. Block diagram of three-leg inverter and SPIM.

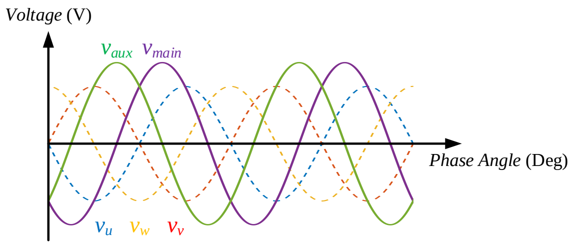

Fig. 3. Output voltages of three-leg inverter for the SPIM drives.

In this paper, the power sharing controller and the modified modulation strategy are suggested to reduce the torque pulsation in the V/f control for SPIM drives. The validation of the proposed methods are demonstrated by simulation and experimental results.

II. Proposed Method for Pulsating Torque Reduction

In general, the auxiliary winding has additional turns, a greater resistance and a lower current when the SPIM is supplied with balanced two-phase voltages. However, if the stator windings are supplied with unbalanced voltages considering impedances in stator windings, the torque pulsation can be reduced. Each stator winding of the SPIM is connected to the three-leg VSI as shown in Fig. 2. The three-leg VSI allows the removal of the self-starting capacitor and supplies unbalanced voltages to reduce the torque pulsation. In the V/f control for SPIM drives, a higher voltage is supplied to the auxiliary winding considering the turns ratio of stator windings [4].

A. Condition for Torque Pulsation Reduction [3]

The equivalent model of the SPIM with asymmetric main and auxiliary windings based on the double revolving field theory [5], [6] is shown in Fig. 4. The average electromagnetic torque T_{em} developed using this model is given by (1) and the peak amplitude of the pulsating torque T_p is given by (2).

$$T_{em}\omega_s = [I_m^2 + (\alpha I_a)^2](R_f - R_b) + 2\alpha I_a I_m (R_f - R_b)\sin\phi, \tag{1}$$

$$T_p\omega_s = \left\{ \frac{[I_m^4 + (\alpha I_a)^4 + 2(\alpha I_a I_m)^2 \cos 2\phi]}{\left[(R_f - R_b)^2 + (X_f - X_b)^2\right]} \right\}^{\frac{1}{2}} \tag{2}$$

where ω_s is the fundamental frequency and ϕ is the phase angle difference between main and auxiliary winding currents. I_m and I_a are main and auxiliary winding currents, respectively. R_f and X_f are resistance and reactance of forward impedances. R_b and X_b are resistance and reactance of backward impedances. α is the effective turns ratio of the auxiliary winding to the main winding.

The main winding voltage V_m and the auxiliary winding voltage V_a can be expressed in terms of currents and impedances in the equivalent model shown in Fig. 4.

$$\mathbf{V}_m = \mathbf{I}_m Z_1 + \mathbf{I}_a Z_2, \tag{3}$$

$$\mathbf{V}_a = \mathbf{I}_m Z_4 + \mathbf{I}_a Z_3 \tag{4}$$

where

$$Z_1 = R_{1m} + R_f + R_b + j(X_{1m} + X_f + X_b) = a_1 + jb_1, \tag{5}$$

$$Z_2 = -j\alpha[(R_f - R_b) + (X_f - X_b)] = a_2 + jb_2, \tag{6}$$

$$Z_3 = R_{1a} + \alpha^2(R_f + R_b) + j[X_{1a} + \alpha^2(X_f + X_b)] = a_3 + jb_3, \tag{7}$$

$$Z_4 = j\alpha[(R_f - R_b) + (X_f - X_b)] = a_4 + jb_4 \tag{8}$$

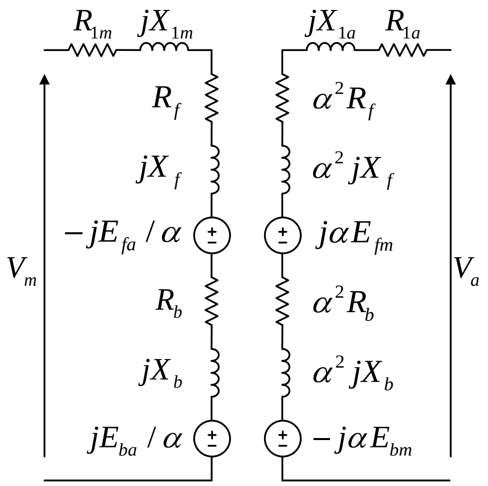

Fig. 4. Double revolving field theory model of SPIM.

According to (1) and (2), the torque is determined by I_m, I_a and ϕ. From (2), the torque pulsation can be eliminated at speeds other than standstill when I_m equals to αI_a and ϕ is 90° as follow.

$$\mathbf{I}_m = \pm j\alpha \mathbf{I}_a \tag{9}$$

Also, T_{em} reaches maximum value for the same I_m and I_a. In other words, it is possible to drive the SPIM with less currents under the same operating condition. The relationship of V_m and V_a is determined from (3), (4) and (9) as follows.

$$V_a = |\mathbf{V}_a| = V_m \left| \frac{Z_3 + \alpha Z_4}{\alpha Z_1 + Z_2} \right| = kV_m, \tag{10}$$

$$k = \sqrt{\frac{(a_3 + \alpha a_4)^2 + (b_3 + \alpha b_4)^2}{(a_2 + \alpha a_1)^2 + (b_2 + \alpha b_1)^2}} \tag{11}$$

Voltage ratio k of (11) with (9) produces circular rotating magnetic field at any operating point and the torque pulsation is eliminated, thus improving the efficiency of the SPIM during variable speed operation. However, the calculation of (11) is complex and contains SPIM parameters. Therefore, it isn't suitable to be applied to the V/f control since SPIM parameters are unknown except for nameplate values. In [7], the relative amplitude relation of two winding voltages is given by (13) instead of (10) and is illustrated in Fig. 5.

$$V_m^* = \frac{V_{rated}}{\omega_{rated}} \omega_s^*, \tag{12}$$

$$V_a^* = \alpha V_m^* \tag{13}$$

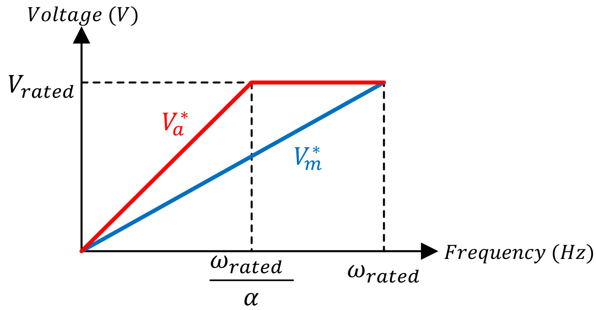

Fig. 5. Reference voltages of V/f control for a SPIM drive.

where V_{rated} and ω_{rated} are the nominal voltage and electrical frequency of the SPIM. ω_s^* is reference electrical frequency for the V/f control. V_m^* and V_a^* are reference voltage amplitudes of the main and auxiliary windings.

The V/f control is a simple variable speed control method in which the stator supply voltage is dependent on the frequency of the applied voltage. For the SPIM drive, the auxiliary winding is supplied with a higher voltage considering the turns ratio α of stator windings, as shown in Fig. 5. The voltage ratio k of (11) is approximately equal to the turns ratio α from impedance matching and winding power balance perspective [8]. So, the voltage ratio of (13) is expected to produce the maximum average torque with reduced torque pulsation. However, in practice, without additional parameter estimations, it is difficult to obtain motor parameters including the turns ratio α except for information on the nameplate. Thus, the V/f control shown in Fig. 5 containing α is also impractical.

B. Proposed V/f Control for SPIM Drive with Pulsating Torque Reduction

To improve simplicity, the proposed V/f control for a SPIM drive determines the voltage ratio and the phase angle difference without motor parameters. Assuming that two winding impedances have the same ratio as α, each of the complex power $\mathbf{S}_m$ and $\mathbf{S}_a$ is expressed from (3) and (4) as follows.

$$\mathbf{S}_m = \mathbf{V}_m\bar{\mathbf{I}}_m \approx \mathbf{I}_m\bar{\mathbf{I}}_m(a_1 + jb_1) + \mathbf{I}_a\bar{\mathbf{I}}_m(a_2 + jb_2), \quad (14)$$

$$\mathbf{S}_a = \mathbf{V}_a\bar{\mathbf{I}}_a \approx \mathbf{I}_a\bar{\mathbf{I}}_a\alpha^2(a_1 + jb_1) - \mathbf{I}_m\bar{\mathbf{I}}_a(a_2 + jb_2) \quad (15)$$

where the bar placed above the complex number means the complex conjugate.

According to these power equations, when the active and reactive powers of stator windings are balanced, stator currents corresponding to (9) are generated and the voltage ratio between two windings becomes α. Then, the air-gap power P_g is expressed as follows [5].

$$P_g = 4I_m^2R_f \quad (16)$$

P_g of (16) contains no alternating power, same as the air-gap power in a symmetric two-phase induction motor. Due to constant air-gap power and symmetric windings in the rotor circuit, the torque is constant similarly to the general V/f control for a three-phase induction motor. Therefore, when the stator circuits consisting of main and auxiliary windings supplies balanced active and reactive powers to the rotor circuit which are symmetric, the torque pulsation can be reduced. In the proposed method, the voltage ratio and phase angle difference between main and auxiliary windings on the stator are determined by power sharing controllers, as shown in Fig. 6, so that the balanced active and reactive powers are supplied to the rotor circuit.

The power sharing controllers used in this paper are similar to $P-V$ and $Q-f$ droop controls which regulate the voltage amplitude for active power sharing and voltage phase angle for reactive power sharing [9]. As shown in Fig. 7, the active power sharing controller

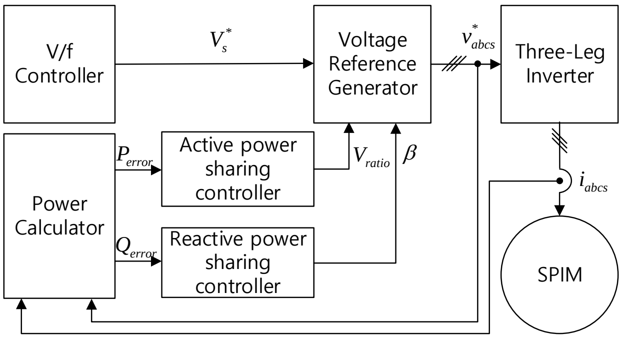

Fig. 6. Block diagram of the proposed method for power sharing

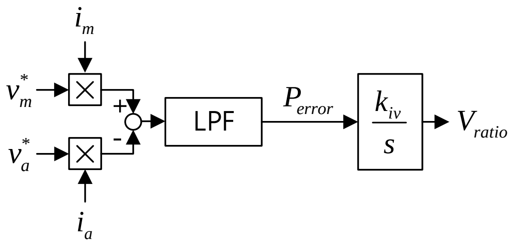

Fig. 7. Block diagram of the active power sharing controller and the active power calculator.

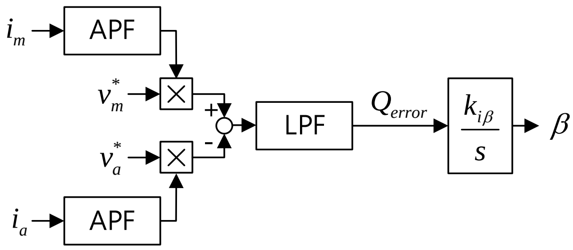

Fig. 8. Block diagram of the reactive power sharing controller and the reactive power calculator.

determines the voltage ratio V_{ratio} from active power difference P_{error}. As shown in Fig. 8, the reactive power sharing controller determines the phase angle difference β from reactive power difference Q_{error}. Respective powers are measured from output voltages and currents of a three-leg VSI, and Low pass filter (LPF) is necessary to eliminate the second harmonic component of stator powers in main and auxiliary windings. All pass filter (APF) is also necessary to generate the required quadrature currents for calculating the reactive power.

Compared to conventional methods, the proposed method doesn't require motor parameters and generates appropriate reference voltages $\boldsymbol{V}_m^*$ and $\boldsymbol{V}_a^*$ for stator powers sharing which reduce the torque pulsation.

III. Modulation Strategy for Proposed V/f Control

For a SPIM driven by a three-leg VSI, reference output voltages should consider V_{ratio} and β which are important for pulsating torque reduction in the proposed method. In [10], as shown in Fig. 9, the voltage phasor diagram shows the modulation scheme. The reference output voltages v_u^*, v_v^* and v_w^* are defined with respect to the middle point of the DC-link voltage and are generated by (17).

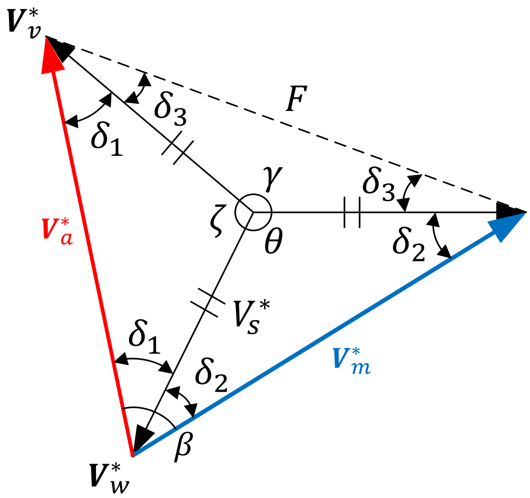

Fig. 9. Voltage phasor diagram for a SPIM drive.

$$\begin{aligned} v_u^* &= V_s^* \cos(\omega_s^* t) \\ v_v^* &= V_s^* \cos(\omega_s^* t + \gamma) \\ v_w^* &= V_s^* \cos(\omega_s^* t - \theta) \end{aligned} \quad (17)$$

where V_s^* is the amplitude of reference output voltage. γ and θ represent the phase angle of v_v^* and v_w^*, respectively.

V_s^*, γ and θ are needed to generate reference output voltages and calculated with (18), (19) and (20) using trigonometry while ω_s^* is predetermined by the speed command.

$$\begin{aligned} \delta_3 &= \frac{\pi}{2} - \beta, \\ V_s^* &= \frac{(V_m^*)^2}{2} \frac{\sqrt{V_{ratio}^2 + 1 - 2V_{ratio}\cos(\beta)}}{\cos\left(\frac{\pi}{2} - \beta\right)} \end{aligned} \quad (18)$$

From Fig. 9, δ_1 and δ_2 are found to be

$$\begin{aligned} \delta_1 &= \cos^{-1}\left(\frac{V_a^*}{2V_s^*}\right), \\ \delta_2 &= \cos^{-1}\left(\frac{V_m^*}{2V_s^*}\right) \end{aligned} \quad (19)$$

Finally, the phase angles γ, θ and ζ are

$$\begin{aligned} \zeta &= \pi - 2\delta_1, \\ \theta &= \pi - 2\delta_2, \\ \gamma &= \pi - 2\delta_3 \end{aligned} \quad (20)$$

From (18), V_s^* is generated by V_m^*, V_{ratio} (or V_a^*) and β. Considering the DC-link voltage utilization, V_m^* of (18) should be appropriately determined depending on V_{ratio} and β. If V_m^* is not proper, V_{ratio} or β is limited with the over-modulation, which is important factor for the proposed method. For example, Fig. 5 shows that V_{ratio} is limited at adjacent rated frequency. Therefore, in this paper, modified modulation method is used for the V/f control with the SPIM. For the modified modulation, V_s^* is predetermined by the relationship between voltage amplitude and frequency, as shown in Fig. 10, which is the same as a general V/f control for three-phase induction motor drives. Fig. 10 corresponds to the V/f controller of Fig. 6 and determines V_s^* according to the frequency.

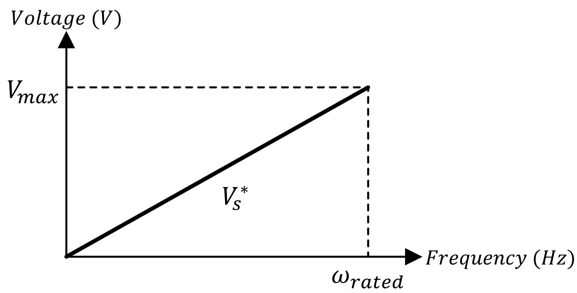

Fig. 10. Reference phase voltage for the general V/f control.

V_{max} is $\frac{V_{dc}}{2}$ considering a three-leg inverter topology for a SPIM drive, and limits V_s^* to prevent the over-modulation.

Similarly, γ and θ are needed to generate v_u^*, v_v^* and v_w^* while V_s^* and ω_s^* are predetermined as shown in Fig. 10. From (18) and (20), γ is expressed as follow.

$$\gamma = 2\beta \quad (21)$$

And (22) is calculated using the Law of Cosines.

$$(V_m^*)^2 = (V_s^*)^2 + (V_s^*)^2 - 2(V_s^*)^2 \cos(\theta) \quad (22)$$

Thus, from (18) and (22), θ becomes the function of V_{ratio} and β as follow.

$$\theta = \cos^{-1}\left(\frac{\cos(2\beta) - 1}{V_{ratio}^2 + 1 - 2V_{ratio}\cos(\beta)} + 1\right) \quad (23)$$

Predetermining V_s^* in advance, modulation strategy is modified for a V/f control with the SPIM. v_u^*, v_v^* and v_w^* are simply determined by (21), (23) and Fig. 10 while maintain V_{ratio} and β in the overall operating region.

IV. Simulation Results

To confirm the effectiveness of the proposed V/f control for a SPIM, conventional and proposed methods were carried out by the simulation using PLECS. The simulation-based results of the proposed V/f control are compared to the corresponding results of the conventional V/f control. The motor parameters used in the simulation are listed in Table I [11].

Fig. 11 and 12 show the simulation results of conventional and proposed methods at the rated frequency with the rated load.

TABLE I
1/4-HP 110-Vrms 60-Hz 4-Pole SPIM parameters

Parameters	Value	Parameters	Value
R_{1m}	2.02 Ω	R_{2m}	4.12 Ω
R_{1a}	7.14 Ω	R_{2a}	5.74 Ω
X_{1m}	2.79 Ω	X_{2m}	2.12 Ω
X_{1a}	3.22 Ω	X_{2a}	2.95 Ω
X_{Mm}	66.8 Ω	α	1.18
X_{Ma}	92.9 Ω	Inertia	1.407×10^{-3} kg-m^2

As simulation results of the conventional V/f control, Fig. 11(a) shows balanced voltages v_m^* and v_a^* with the constant amplitude 110 V $\left(= V_{dc}/\sqrt{2}\right)$ considering the

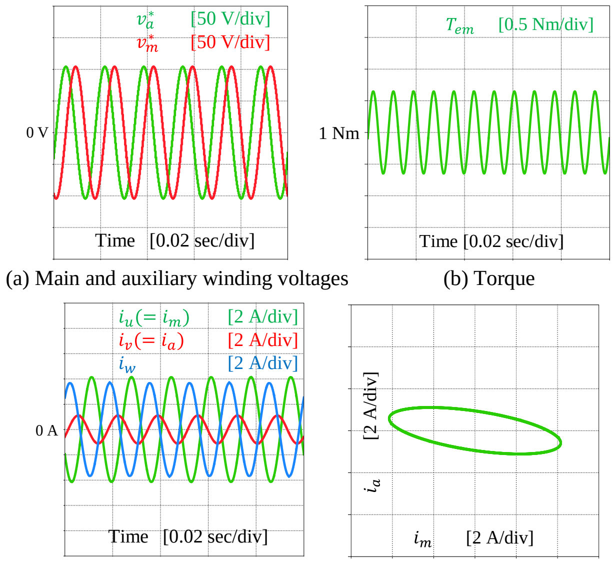

(a) Main and auxiliary winding voltages (b) Torque

(c) Output currents of three-leg VSI (d) Stator current trajectory

Fig. 11. Simulation results of the conventional V/f control

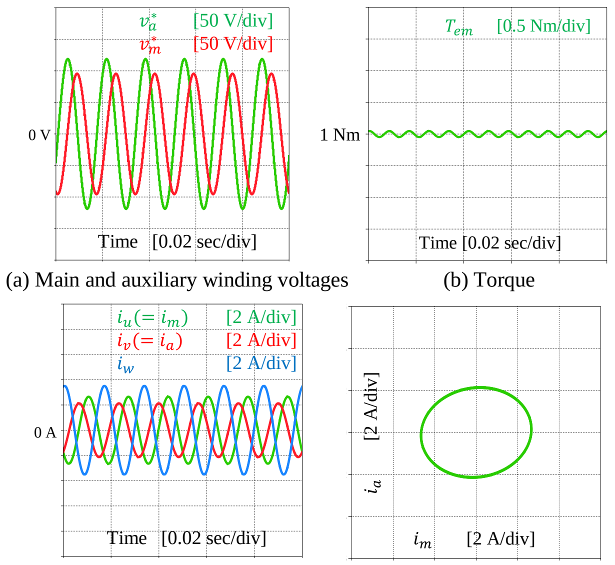

(a) Main and auxiliary winding voltages (b) Torque

(c) Output currents of three-leg VSI (d) Stator current trajectory

Fig. 12. Simulation results of the proposed V/f control

linear modulation range of a three-leg VSI for the SPIM drive, and V_s^* is 77 V$(= V_{dc}/2)$ determined by V/f ratio shown in Fig. 10. i_m and i_a in Fig. 11(c) are unbalanced currents with peak amplitudes of 4.16 A and 1.11 A. Stator current trajectory is elliptical as shown in Fig. 11(d), but i_m is too high when compared to αi_a. This results in the torque pulsation of 0.65 Nm in Fig. 11(b).

As simulation results of the proposed V/f control, Fig. 12(a) shows unbalanced voltages v_m^* and v_a^* adjusted by power sharing controllers, but V_s^* is same as that of the conventional V/f control because the modulation strategy is identical in both methods. i_m and i_a in Fig. 11(c) are also unbalanced currents with peak amplitudes of 2.66 A and 2.14 A, but stator currents are relatively low compared to Fig. 11(c). Stator current trajectory is appropriate because current amplitude ratio of i_m and i_a is 1.24 with error rate 5% $\left(= \left|\frac{i_m}{\alpha i_a} - 1\right|\right)$. As a result, torque pulsation is reduced as shown in Fig. 12(b). The amplitude of the torque pulsation is 0.05 Nm reduced 92% from torque pulsation shown in Fig 11(b). In practice, as shown in Table I, the auxiliary winding impedance is not exactly α times the main winding impedance. Nevertheless, proposed method significantly reduces the torque pulsation.

V. EXPERIMENTAL RESULTS

In this section, experimental results will be shown to verify the proposed method using a three-leg VSI. The structure of the experimental setup is depicted in Fig. 2, and the asymmetrical SPIM removed a capacitor in a capacitor-start induction motor with a rating of 2.2 kW, 220 Vrms, 18.7 Arms, 60 Hz, 4 P, 1765 r/min is used for the test. The experimental setup doesn't include a torque meter and thus experimental results show output currents of the three-leg VSI according to load torques, as shown in Fig. 13 and 14.

Fig. 13 shows the experiment results of the conventional method. At no-load torque, the peak current of i_m is about 18 A which is considerably high compared to the rated current, as shown Fig. 13(a). To improve the efficiency, it is required to reduce the no-load current. At 50% load torque, the peak current of i_m is already close to the rated current as shown Fig. 13(b).

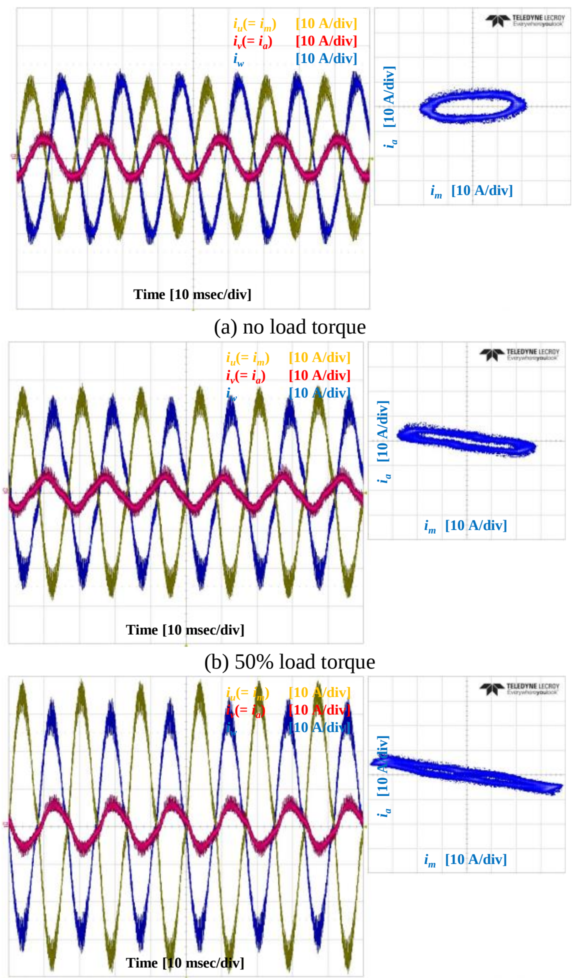

(a) no load torque

(b) 50% load torque

(c) 100% load torque

Fig. 13. Experiment results of conventional V/f control

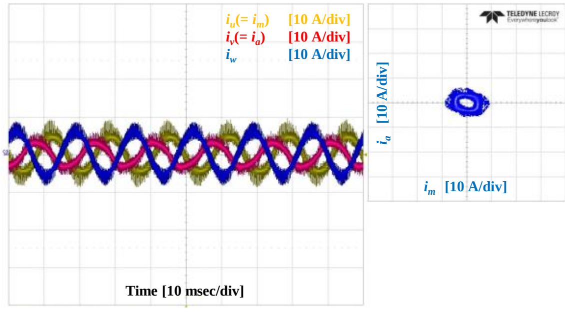

(a) no load torque

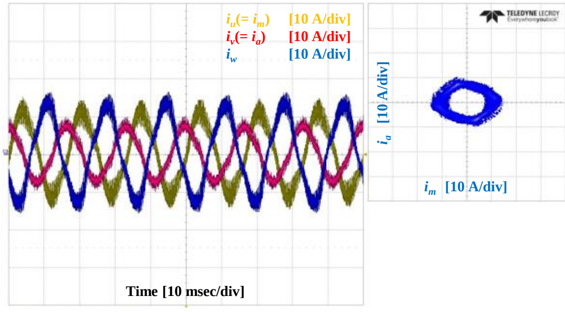

(b) 50% load torque

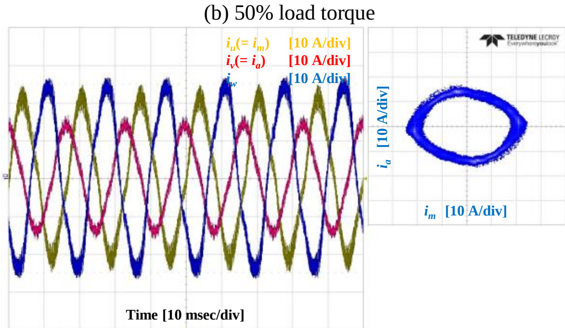

(c) 100% load torque

Fig. 14. Experiment results of proposed V/f control

High current of about 35 A exceeding the rated current occurs at 100% load torque. Moreover, since i_m and i_a in Fig. 13 don't sufficiently satisfy the condition for pulsating torque elimination corresponding to (9), the torque pulsation occurs significantly. Similar to the simulation result of Fig. 11, i_m in Fig. 13 is also too high compared to i_a.

Fig. 14 shows the experiment results of the proposed method. The current amplitude in the proposed method is proportional to the load torque, same as the general V/f control. The proposed method drives the SPIM from no-load torque to the rated torque without over current. In particular, regardless of load torques, current amplitude ratio is relatively constant and the phase angle difference between main and auxiliary winding currents is almost close to $90°$ compared to stator currents of the conventional method in Fig 13. Consequently, the proposed method reduces the torque pulsation and currents with less noise and less loss. The effectiveness of the proposed V/f control is confirmed with amplitude and phase angle difference of stator currents compared to results of the conventional V/f control.

VI. Conclusions

This paper has presented the proposed V/f control reducing the torque pulsation for the SPIM drive. The proposed method adds the power sharing controller to the existing V/f control. For sharing active and reactive powers of each winding, power sharing controllers adjust the voltage ratio and the phase angle difference between two stator windings. A three-leg VSI supplies two winding voltages corresponding to line-to-line voltages and the modified modulation strategy is used to generate output voltages suitable to a three-leg VSI and a V/f control for the SPIM drive. With the proposed V/f control method, torque pulsation and stator currents can be reduced compared to the conventional method. The effectiveness of the proposed method was verified through simulation and experiment results.

References

[1] P. C. Krause, Analysis of Electric Machinery and Drive Systems, Wiley-IEEE Press, 2002..

[2] F. Blaabjerg, F. Lungeanu, K. Skaug and M. Tonnes, "Two-phase induction motor drives," in IEEE Industry Applications Magazine, vol. 10, no. 4, pp. 24-32, July-Aug. 2004.

[3] M. N. Almani, G. A. Hussain and A. A. Zaher, "An Improved Technique for Energy-Efficient Starting and Operating Control of Single Phase Induction Motors," in IEEE Access, vol. 9, pp. 12446-12462, 2021.

[4] Ch. Charumit, V. Kinnares, "Carrier-based unbalanced phase voltage space vector PWM strategy for asymmetrical parameter type two-phase induction motor drives," Electric Power Systems Research, Volume 79, Issue 7, 2009, pp. 1127-1135.

[5] W. J. Morrill, "The Revolving Field Theory of the Capacitor Motor," in Transactions of the American Institute of Electrical Engineers, vol. 48, no. 2, pp. 614-629, April 1929.

[6] P. C. Sen, Principles of Electric Machines & Power Electronics, John Wiley & Sons, 2013.

[7] S. Sinthusonthishat and N. Chuladaycha. "A Simplified Modulation Strategy for Three-leg Voltage Source Inverter Fed Unsymmetrical Two-winding Induction Motor" Journal of Electrical Engineering & Technology, vol.8, no.6, pp.1337-1344, 2013.

[8] D. G. Holmes and A. Kotsopoulos, "Variable speed control of single and two phase induction motors using a three phase voltage source inverter," Conference Record of the 1993 IEEE Industry Applications Conference Twenty-Eighth IAS Annual Meeting, Toronto, ON, Canada, 1993, pp. 613-620 vol.1.

[9] Y. Han, H. Li, P. Shen, E. A. A. Coelho and J. M. Guerrero, "Review of Active and Reactive Power Sharing Strategies in Hierarchical Controlled Microgrids," in IEEE Transactions on Power Electronics, vol. 32, no. 3, pp. 2427-2451, March 2017.

[10] E. R. Benedict and T. A. Lipo, "Improved PWM modulation for a permanent-split capacitor motor," Conference Record of the 2000 IEEE Industry Applications Conference. Thirty-Fifth IAS Annual Meeting and World Conference on Industrial Applications of Electrical Energy (Cat. No.00CH37129), Rome, Italy, 2000, pp. 2004-2010 vol.3.

[11] P. C. Krause, "Simulation of Unsymmetrical 2-Phase Induction Machines," in IEEE Transactions on Power Apparatus and Systems, vol. 84, no. 11, pp. 1025-1037, Nov. 1965.